

# Isospin Dynamics in Heavy Ion Collisions

M.Di Toro

*Laboratori Nazionali del Sud INFN,  
Via S.Sofia 62, 95123 Catania, Italy,  
and Physics-Astronomy Dept., University of Catania,  
E-mail: [ditoro@lns.infn.it](mailto:ditoro@lns.infn.it)*

Some isospin dynamics results in heavy ion collisions from low to relativistic energies obtained through transport approaches, largely inspired by David M.Brink, are reviewed. At very low energies, just above the Coulomb barrier, the stimulating implications of the prompt dipole radiation in dissipative collisions of ions with large isospin asymmetries are discussed. We pass then to the very rich phenomenology of isospin effects on heavy ion reactions at intermediate energies (few  $A$  GeV range). We show that it can allow a “direct” study of the covariant structure of the isovector interaction in the hadron medium. We work within a relativistic transport frame, beyond a cascade picture, consistently derived from effective Lagrangians, where isospin effects are accounted for in the mean field and collision terms. Rather sensitive observables are proposed from collective flows (“differential” flows) and from pion/kaon production ( $\pi^-/\pi^+$ ,  $K^0/K^+$  yields). For the latter point relevant non-equilibrium effects are stressed. The possibility of the transition to a mixed hadron-quark phase, at high baryon and isospin density, is finally suggested. Some signatures could come from an expected “neutron trapping” effect. The importance of *violent* collision experiments with radioactive beams, from few  $AMeV$  to few  $AGeV$ , is stressed.

## I. INTRODUCTION: THE DAVID LEGACY

It is a great pleasure and honor to contribute to this special day devoted to celebrate the 75th anniversary of David Brink. After many years of acquaintance and collaboration I would like to state a few points I mostly got from him: 1.) The Mean Field “moves” the world, particularly true in nuclear dynamics, as I will show in examples discussed here; 2.) The role of relativity in nuclear structure and reactions; 3.) Play always a deep attention to the suggestions of young people; 4.) Follow a “sensible” behaviour towards the political choices, i.e. try to change something only when you can count on something better. Here of course I will focus on the physics part showing a series of results broadly inspired by the David ideas.

In the last years the isospin dynamics has gained a lot of interest, as we can see from the development of new heavy ion facilities (radioactive beams), for the unique possibilities of probing the isovector in medium interaction far from saturation, relevant for the structure of unstable elements as well as for nuclear astrophysics see the recent reviews [1, 2].

Here I will show some selected results of the mean field transport approach in a wide energy range, from few  $AMeV$  to few  $AGeV$ , in non-relativistic and relativistic frames. At low energies I will discuss the isospin equilibration in dissipative collisions, fusion and deep-inelastic, through a related observable, the Prompt Collective Dipole Radiation. At high energies I will shortly present isospin effects on collective flows, on particle production and finally on the transition to a mixed hadron-quark phase at high baryon density.

## II. THE PROMPT DIPOLE $\gamma$ -RAY EMISSION

The possibility of an entrance channel bremsstrahlung dipole radiation due to an initial different  $N/Z$  distribution was suggested at the beginning of the nineties [3, 4], largely inspired by David discussions. At that time a large debate was present on the disappearing of *Hot Giant Dipole Resonances* in fusion reactions. David was suggesting the simple argument that a *GDR* needs time to be built in a hot compound nucleus, meanwhile the system will cool down by neutron emission and the *GDR* photons will show up at lower temperature. The natural consequence suggested in [3] was that we would expect a new dipole emission, in addition to the statistical one, if some pre-compound collective dipole mode is present. After several experimental evidences, in fusion as well as in deep-inelastic reactions [5, 6, 7, 8, 9] we have now a good understanding of the process and stimulating new perspectives from the use of radioactive beams.

During the charge equilibration process taking place in the first stages of dissipative reactions between colliding ions with different  $N/Z$  ratios, a large amplitude dipole collective motion develops in the composite dinuclear system, the so-called dynamical dipole mode. This collective dipole gives rise to a prompt  $\gamma$ -ray emission which depends: i) on the absolute value of the initial dipole moment

$$D(t=0) = \frac{NZ}{A} |R_Z(t=0) - R_N(t=0)| = \frac{R_p + R_t}{A} Z_p Z_t \left| \left(\frac{N}{Z}\right)_t - \left(\frac{N}{Z}\right)_p \right|, \quad (1)$$

being  $R_Z$  and  $R_N$  the center of mass of protons and of neutrons respectively, while  $R_p$  and  $R_t$  are the projectile and target radii; ii) on the fusion/deep-inelastic dynamics; iii) on the symmetry term, below saturation, that is

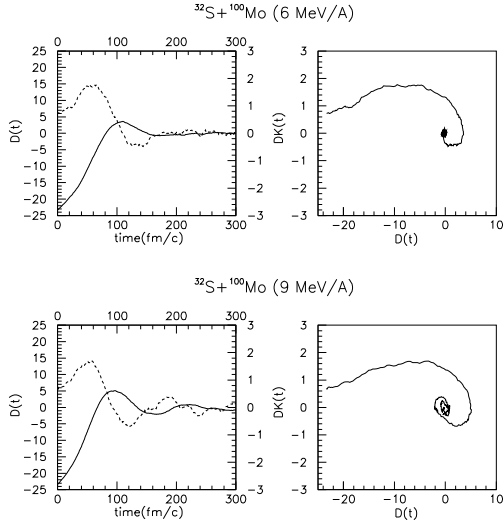


FIG. 1: The time evolution of the dipole mode in  $r$ -space  $D(t)$  (solid lines) and  $p$ -space  $DK(t)$  (dashed lines, in  $fm^{-1}$ ) and the correlation  $DK(t) - D(t)$  at incident energy of 6  $AMeV$  and 9  $AMeV$  for  $b = 2fm$ .

acting as a restoring force.

A detailed description is obtained in a microscopic approach based on semiclassical transport equations, of Vlasov type, introduced in the nuclear dynamics in collaboration with David [10], where mean field and two-body collisions are treated in a self-consistent way, see details in [11]. Realistic effective interactions of Skyrme type are used. The numerical accuracy of the transport code has been largely improved in order to have reliable results also at low energies, just above the threshold for fusion reactions [12, 13]. The resulting physical picture is in good agreement with quantum Time-Dependent-Hartree-Fock calculation [14]. In particular we can study in detail how a collective dipole oscillation develops in the entrance channel [13].

First, during the *approaching phase*, the two partners, overcoming the Coulomb barrier, still keep their own response. Then follows a *dinuclear phase* where the relative motion energy, due to the nucleon exchange, is converted in thermal motion and in the collective energy of the dinuclear mean field. In fact the composite system is not fully equilibrated and manifests, as a whole, a large amplitude dipole collective motion. Finally thermally equilibrated reaction products are formed, with consequent statistical particle/radiation emissions.

We present here some results for the  $^{32}S + ^{100}Mo$  ( $N/Z$  asymmetric) reaction at 6 and 9  $AMeV$ , recently studied vs. the “symmetric”  $^{36}S + ^{96}Mo$  counterpart in ref.[9]. In Fig.1 (left columns) we draw the time evolution for  $b = 2fm$  of the dipole moment in the  $r$ -space (solid lines),  $D(t) = \frac{NZ}{A}X(t)$  and in  $p$ -space (dashed lines),  $DK(t) = \Pi/\hbar$ , where  $\Pi = \frac{NZ}{A}(\frac{P_p}{Z} - \frac{P_n}{N})$ , with  $P_p$  ( $P_n$ ) center of mass in momentum space for protons (neutrons), is just the canonically conjugate momentum

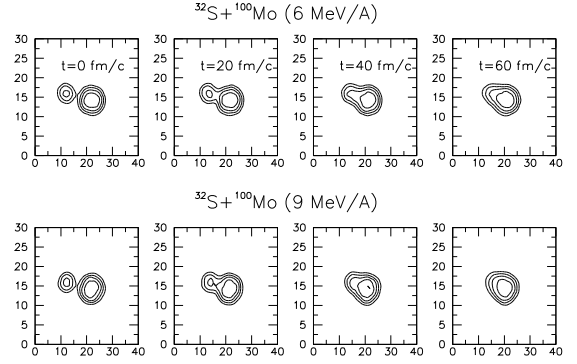


FIG. 2: Density plots of the neck dynamics for the  $^{32}S + ^{100}Mo$  system at incident energy of 6  $AMeV$  and 9  $AMeV$ .

of the  $X$  coordinate, see [13, 14, 15]. On the right hand side columns we show the corresponding correlation  $DK(t) - D(t)$  in the phase space. We choose the origin of time at the beginning of the *dinuclear* phase. The nice “spiral-correlation” clearly denotes the collective nature of the mode. From Fig.1 we note that the “spiral-correlation” starts when the initial dipole moment  $D(t = 0)$ , the geometrical value at the touching point, is already largely quenched. This is the reason why the dinucleus dipole yield is not simply given by the “static” estimation but the reaction dynamics has a large influence on it.

A clear energy dependence of the dynamical dipole mode is evidenced with a net increase when we pass from 6  $AMeV$  to 9  $AMeV$ . A possible explanation of this effect is due to the fact that at lower energy, just above the Coulomb barrier, a longer transition to a dinuclear configuration is required which hinders the isovector collective response. From Fig.2 a slower dynamics of the neck during the first 40  $fm/c$  – 60  $fm/c$  from the touching configuration is observed at 6  $AMeV$ . When the collective dipole response sets in the charge is already partially equilibrated via random nucleon exchange.

The bremsstrahlung spectra shown in Fig.3 support this interpretation.

In fact from the dipole evolution given from the Vlasov transport we can directly apply a bremsstrahlung (“*bremss*”) approach [15] to estimate the “direct” photon emission probability ( $E_\gamma = \hbar\omega$ ):

$$\frac{dP}{dE_\gamma} = \frac{2e^2}{3\pi\hbar c^3 E_\gamma} |D''(\omega)|^2, \quad (2)$$

where  $D''(\omega)$  is the Fourier transform of the dipole acceleration  $D''(t)$ . We remark that in this way it is possible to evaluate, in *absolute* values, the corresponding pre-equilibrium photon emission. In the same Fig.3 we show statistical *GDR* emissions from the final excited residue. We see that at the higher energy the prompt emission represents a large fraction of the total dipole radiation.

In the Table we report the present status of the Dynamical Dipole data, obtained from fusion reactions.. We

TABLE I: The percent increase of the intensity in the linearized  $\gamma$ -ray spectra at the compound nucleus GDR energy region (the energy integration limits are given in the parenthesis), the compound nucleus excitation energy, the initial dipole moment  $D(t=0)$  and the initial mass asymmetry  $\Delta$  for each reaction.

Reaction	Increase (%)	$E^*$ (MeV)	$D(t=0)$ (fm)	$\Delta$	Ref
$^{40}\text{Ca}+^{100}\text{Mo}$	16 (8,18)	71	22.1	0.15	[5]
$^{36}\text{S}+^{104}\text{Pd}$		71	0.5	0.17	
$^{16}\text{O}+^{98}\text{Mo}$	36 (8,20)	110	8.4	0.29	[6]
$^{48}\text{Ti}+^{64}\text{Ni}$		110	5.2	0.05	
$^{32}\text{S}+^{100}\text{Mo}$	$1.6 \pm 2.0$ (8,21)	117	18.2	0.19	[9]
$^{36}\text{S}+^{96}\text{Mo}$		117	1.7	0.16	
$^{32}\text{S}+^{100}\text{Mo}$	25 (8,21)	173.5	18.2	0.19	[7]
$^{36}\text{S}+^{96}\text{Mo}$		173.5	1.7	0.16	

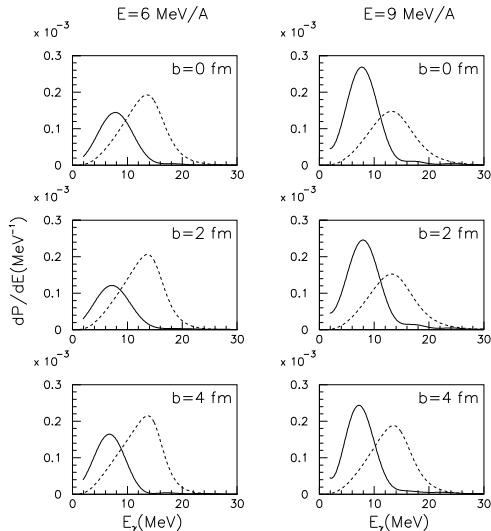


FIG. 3: The bremsstrahlung spectra for the  $^{32}\text{S} + ^{100}\text{Mo}$  system at incident energy of 6 A MeV and 9 A MeV (solid line) and the first step statistical spectrum (dashed line) for three impact parameters.

note the dependence of the extra strength on the interplay between initial dipole moment and initial mass asymmetry: this clearly indicates the relevance of the fusion dynamics.

We must add a couple of comments of interest for the experimental selection of the Dynamical Dipole: i) The centroid is always shifted to lower energies (large deformation of the dinucleus); ii) A clear angular anisotropy should be present since the prompt mode has a definite axis of oscillation (on the reaction plane) at variance with the statistical GDR. At higher beam energies we expect a further decrease of the direct dipole radiation for two main reasons both due to the increasing importance of hard NN collisions: i) a larger fast nucleon emission that will equilibrate the isospin before the collective dipole starts up; ii) a larger damping of the collective mode. This has been observed in ref.[8] and more expts. are planned [16].

Before closing I would like to note two interesting

developments for future experiments with radioactive beams:

- The prompt dipole radiation represents a nice cooling mechanism on the fusion path. It could be a way to pass from a *warm* to a *cold* fusion in the synthesis of heavy elements with a noticeable increase of the *survival* probability, [17].
- The use of unstable neutron rich projectiles would largely increase the effect allowing a detailed study of the symmetry potential, below saturation, responsible of the restoring force of the dipole oscillation [18]

### III. ISOSPIN PHYSICS IN A COVARIANT APPROACH

We move now to a relativistic framework for the description of the isovector part of the effective interaction. I will focus then the attention on relativistic heavy ion collisions, that provide a unique terrestrial opportunity to probe the in-medium nuclear interaction in high density and high momentum regions. An effective Lagrangian approach to the hadron interacting system is extended to the isospin degree of freedom: within the same frame equilibrium properties ( $EoS$ , [19]) and transport dynamics ([20, 21]) can be consistently derived. Within a covariant picture of the nuclear mean field, for the description of the symmetry energy at saturation ( $a_4$  parameter of the Weizsäcker mass formula) (in a sense equivalent to the  $a_1$  parameter for the iso-scalar part), extracted in the range from 28 to 36 MeV, there are different possibilities: (a) considering only the Lorentz vector  $\rho$  mesonic field, and (b) both, the vector  $\rho$  (repulsive) and scalar  $\delta$  (attractive) effective fields [22, 23, 24]. The latter corresponds to the two strong effective  $\omega$  (repulsive) and  $\sigma$  (attractive) mesonic fields of the iso-scalar sector. We get a transparent form [2, 23]:

$$E_{sym} = \frac{1}{6} \frac{k_F^2}{E_F^*} + \frac{1}{2} \left[ f_\rho - f_\delta \left( \frac{m^*}{E_F^*} \right)^2 \right] \rho_B, \quad (3)$$

with  $E_F^* \equiv \sqrt{k_F^2 + m^{*2}}$ .

Once the  $a_4$  empirical value is fixed from the  $\rho - \delta$  balance, important effects at supra-normal densities appear due to the introduction of the effective  $\delta$  field. In fact the presence of an isovector scalar field is increasing the repulsive  $\rho$ -meson contribution at high baryon densities [2, 23] via a pure relativistic mechanism, due to the different Lorentz properties of these fields (the vector  $\rho$  field grows with baryon density whereas the scalar  $\delta$  field is suppressed by the scalar density). Dynamical, non-equilibrium, effects can be more sensitive to such “fine structure” of the isovector interaction. We will see the vector couplings give  $\gamma$ -boosted Lorentz forces, and so we expect a larger isospin dependence of the high energy nucleon propagation. Moreover, the scalar  $\delta$  field naturally leads to an effective (*Dirac*) mass splitting between protons and neutrons [2, 22, 23, 24, 25, 26], with influence on nucleon emissions and flows [27, 28]. In order to explore the symmetry energy at supra-normal densities one has to select signals directly emitted from the early non-equilibrium high density stage of the heavy ion collision. A transverse momentum analysis is important in order to select the high density source [29, 30]. The description of the mean field is important, since nucleons and resonances are *dressed* by the self-energies. This will directly affect the energy balance (threshold and phase space) of the inelastic channels.

### Relativistic Transport

The starting point is a simple phenomenological version of the Non-Linear (with respect to the iso-scalar, Lorentz scalar  $\sigma$  field) Walecka model which corresponds to the Hartree or Relativistic Mean Field (*RMF*) approximation within the Quantum-Hadrodynamics [19]. According to this model the baryons (protons and neutrons) are described by an effective Dirac equation  $(\gamma_\mu k^{*\mu} - M^*)\Psi(x) = 0$ , whereas the mesons, which generate the classical mean field, are characterized by corresponding covariant equations of motion. The presence of the hadronic medium modifies the masses and momenta of the hadrons, i.e.  $M^* = M + \Sigma_s$  (effective masses),  $k^{*\mu} = k^\mu - \Sigma^\mu$  (kinetic momenta), where we have introduced the scalar and vector self-energies  $\Sigma_s$ ,  $\Sigma^\mu$ . For asymmetric matter the self-energies are different for protons and neutrons, depending on the isovector meson contributions. We will call the corresponding models as  $NL\rho$  and  $NL\rho\delta$ , respectively, and just  $NL$  the case without isovector interactions. We will show also some results with Density Dependent couplings, in order to probe effects which go beyond the *RMF* picture. For the more general  $NL\rho\delta$  case the self-energies of protons and neutrons read:

$$\begin{aligned}\Sigma_s(p, n) &= -f_\sigma \sigma(\rho_s) \pm f_\delta \rho_{s3}, \\ \Sigma^\mu(p, n) &= f_\omega j^\mu \mp f_\rho j_3^\mu,\end{aligned}\quad (4)$$

(upper signs for neutrons), where  $\rho_s = \rho_{sp} + \rho_{sn}$ ,  $j^\alpha = j_p^\alpha + j_n^\alpha$ ,  $\rho_{s3} = \rho_{sp} - \rho_{sn}$ ,  $j_3^\alpha = j_p^\alpha - j_n^\alpha$  are the total and isospin scalar densities and currents and  $f_{\sigma, \omega, \rho, \delta}$  are the coupling constants of the various mesonic fields.  $\sigma(\rho_s)$  is the solution of the non linear equation for the  $\sigma$  field [2, 23].

For the description of heavy ion collisions we solve the covariant transport equation of the Boltzmann type [20, 21] within the Relativistic Landau Vlasov (*RLV*) method, phase-space Gaussian test particles [31], and applying a Monte-Carlo procedure for the hard hadron collisions. The collision term includes elastic and inelastic processes involving the production/absorption of the  $\Delta(1232\text{MeV})$  and  $N^*(1440\text{MeV})$  resonances as well as their decays into pion channels, [32, 33].

A relativistic kinetic equation can be obtained from nucleon Wigner Function dynamics derived from the effective Dirac equation [21]. The neutron/proton Wigner functions are expanded in terms of components with definite transformation properties. Consistently with the effective fields included in our minimal model one can limit the expansion to scalar and vector parts  $\hat{F}^{(i)}(x, p) = F_S^{(i)}(x, p) + \gamma_\mu F^{(i)\mu}(x, p)$ ,  $i = n, p$ . We get after some algebra a transport equation of Vlasov type for the scalar part  $f_i(x, p^*) \equiv F_S^i/M_i^*$ ;  $\{p_{\mu i}^* \partial^\mu + [p_{\nu i}^* F_i^{\mu\nu} + M_i^* (\partial^\mu M_i^*)] \partial_\mu^{p^*}\} f_i(x, p^*) = 0$ , with the field tensors  $F_i^{\mu\nu} \equiv \partial^\mu p_i^{*\nu} - \partial^\nu p_i^{*\mu}$ . The trajectories of test particles obey to the following equation of motion:

$$\begin{aligned}\frac{d}{d\tau} x_i^\mu &= \frac{p_i^*(\tau)}{M_i^*(x)}, \\ \frac{d}{d\tau} p_i^{*\mu} &= \frac{p_{i\nu}^*(\tau)}{M_i^*(x)} F_i^{\mu\nu}(x_i(\tau)) + \partial^\mu M_i^*(x).\end{aligned}\quad (5)$$

In order to have an idea of the dynamical effects of the covariant nature of the interacting fields, we write down, with some approximations, the “force” acting on a particle. Since we are interested in isospin contributions we will take into account only the isovector part of the interaction [34]:

$$\begin{aligned}\frac{d\vec{p}_i^*}{d\tau} &= \pm f_\rho \frac{p_{i\nu}^*}{M_i^*} \left[ \vec{\nabla} J_3^\nu - \partial^\nu \vec{J}_3 \right] \mp f_\delta \nabla \rho_{s3} \\ &\approx \pm f_\rho \frac{E_i^*}{M_i^*} \vec{\nabla} \rho_3 \mp f_\delta \vec{\nabla} \rho_{s3}, \quad (p/n)\end{aligned}\quad (6)$$

The Lorentz force (first term of Eq.(6) shows a  $\gamma = \frac{E_i^*}{M_i^*}$  boosting of the vector coupling, while from the second term we expect a  $\gamma$ -quenched  $\delta$  contribution. We remark that the Lorentz-like force is absent in the non-relativistic Vlasov transport equation discussed before. This nicely shows the qualitative different dynamics of a fully relativistic approach. You cannot get it just inserting a relativistic kinematics in the classical transport equations.

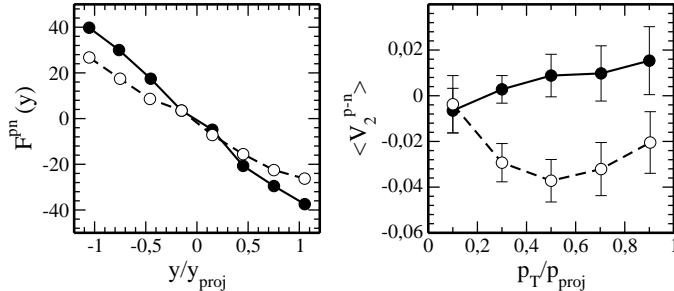


FIG. 4: Differential neutron-proton flows for the  $^{132}\text{Sn} + ^{124}\text{Sn}$  reaction at 1.5 AGeV ( $b=6\text{fm}$ ) from the three different models for the isovector mean fields. Top: Transverse Flows. Bottom: Elliptic Flows. Full circles and solid line:  $NL\rho\delta$ . Open circles and dashed line:  $NL\rho$ .

#### IV. COLLECTIVE FLOWS

The flow observables can be seen respectively as the first and second coefficients of a Fourier expansion of the azimuthal distribution [35]:  $\frac{dN}{d\phi}(y, p_t) \approx 1 + 2V_1\cos(\phi) + 2V_2\cos(2\phi)$  where  $p_t = \sqrt{p_x^2 + p_y^2}$  is the transverse momentum and  $y$  the rapidity along beam direction. The transverse flow can be also expressed as:  $V_1(y, p_t) = \langle \frac{p_x}{p_t} \rangle$ . The sideward (transverse) flow is a deflection of forwards and backwards moving particles, within the reaction plane. The second coefficient of the expansion defines the elliptic flow given by  $V_2(y, p_t) = \langle \frac{p_x^2 - p_y^2}{p_t^2} \rangle$ . It measures the competition between in-plane and out-of-plane emissions. The sign of  $V_2$  indicates the azimuthal anisotropy of emission: particles can be preferentially emitted either in the reaction plane ( $V_2 > 0$ ) or out-of-plane (*squeeze-out*,  $V_2 < 0$ ) [35, 36]. The  $p_t$ -dependence of  $V_2$  is very sensitive to the high density behavior of the *EoS* since highly energetic particles ( $p_t \geq 0.5$ ) originate from the initial compressed and out-of-equilibrium phase of the collision. For the isospin effects the neutron-proton *differential* flows  $V_{1,2}^{(n-p)}(y, p_t) \equiv V_{1,2}^n(y, p_t) - V_{1,2}^p(y, p_t)$  have been suggested as very useful probes of the isovector part of the *EoS* since they appear rather insensitive to the isoscalar potential and to the in medium nuclear cross sections, [37, 38].

In heavy-ion collisions around 1 AGeV with radioactive beams, due to the large counterstreaming nuclear currents, one may exploit the different Lorentz nature of a scalar and a vector field, see the different  $\gamma$ -boosting in the local force, Eq.(6). In Fig.4 transverse and elliptic differential flows are shown for the  $^{132}\text{Sn} + ^{124}\text{Sn}$  reaction at 1.5 AGeV ( $b = 6\text{fm}$ ), that likely could be studied with the new planned radioactive beam facilities at intermediate energies, [34]. The effect of the different structure of the isovector channel is clear. Particularly

evident is the splitting in the high  $p_t$  region of the elliptic flow. In the  $(\rho + \delta)$  dynamics the high- $p_t$  neutrons show a much larger *squeeze-out*. This is fully consistent with an early emission (more spectator shadowing) due to the larger repulsive  $\rho$ -field. The  $V_2$  observable, which is a good *chronometer* of the reaction dynamics, appears to be particularly sensitive to the Lorentz structure of the effective interaction. We expect similar effects, even enhanced, from the measurements of differential flows for light isobars, like  $^3\text{H}$  vs.  $^3\text{He}$ .

#### V. ISOSPIN EFFECTS ON SUB-THRESHOLD KAON PRODUCTION AT INTERMEDIATE ENERGIES

Particle production represent a useful tool to constrain the poorly known high density behaviour of the nuclear equation of state (*EoS*) [39, 40]. In particular pion and (subthreshold) kaon productions have been extensively investigated leading to the conclusion of a soft behaviour of the *EoS* at high densities, [41, 42]. Kaons ( $K^0, K^+$ ) appear as particularly sensitive probes since they are produced in the high density phase almost without subsequent reabsorption effects [41]. At variance, antikaons ( $\bar{K}^0, \bar{K}^-$ ) are strongly coupled to the hadronic medium through strangeness exchange reactions [41, 43]. Here we show that the isospin dependence of the  $K^{0,+}$  production can be also used to probe the isovector part of the *EoS*: we propose the  $K^0/K^+$  yield ratio as a good observable to constrain the high density behavior of the symmetry energy,  $E_{\text{sym}}$ , [1, 2].

Using our *RMF* transport model we analyze pion and kaon production in central  $^{197}\text{Au} + ^{197}\text{Au}$  collisions in the 0.8 – 1.8 AGeV beam energy range, with different effective field choices for  $E_{\text{sym}}$ . We will compare results of three Lagrangians with constant nucleon-meson couplings (*NL...* type, see before) and one with density dependent couplings (*DDF*, see [24]), recently suggested for better nucleonic properties of neutron stars [45]. In the *DDF* model the  $f_\rho$  is exponentially decreasing with density, resulting in a rather “soft” symmetry term at high density. In order to isolate the sensitivity to the isovector components we use models showing the same “soft” *EoS* for symmetric matter.

Pions are produced via the decay of the  $\Delta(1232)$  resonance and can contribute to the kaon yield through collisions with baryons:  $\pi B \rightarrow YK$ . All these processes are treated within a relativistic transport model including an hadron mean field propagation. The latter point, which goes beyond the “collision cascade” picture, is essential for particle production yields since it directly affects the energy balance of the inelastic channels.

Fig. 5 reports the temporal evolution of  $\Delta^{\pm,0,++}$  resonances and pions ( $\pi^{\pm,0}$ ) and kaons ( $K^{+,0}$ ) for central Au+Au collisions at 1 AGeV. It is clear that, while the pion yield freezes out at times of the order of 50 fm/c, i.e. at the final stage of the reaction (and at low densi-

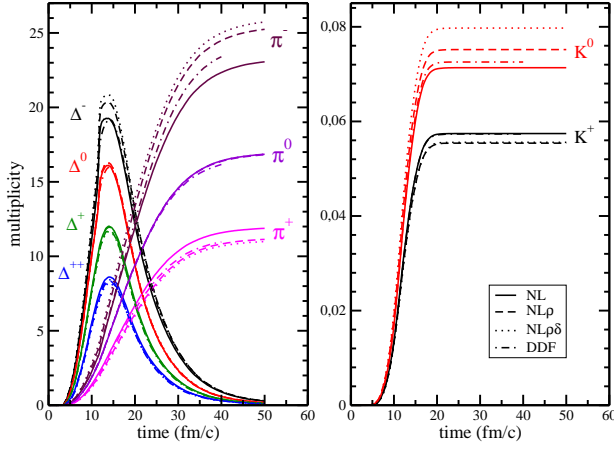


FIG. 5: Time evolution of the  $\Delta^{\pm,0,++}$  resonances and pions  $\pi^{\pm,0}$  (left), and kaons  $K^{0,+}$  (right) for a central ( $b = 0$  fm) impact parameter). Au+Au collision at 1 AGeV incident energy. Transport calculation using the  $NL$ ,  $NL\rho$ ,  $NL\rho\delta$  and  $DDF$  models for the iso-vector part of the nuclear  $EoS$  are shown.

ties), kaon production occur within the very early stage of the reaction, and the yield saturates at around  $20 fm/c$ . Kaons are then suitable to probe the high density phase of nuclear matter. From Fig. 5 we see that the pion results are weakly dependent on the isospin part of the nuclear mean field. However, a slight increase (decrease) in the  $\pi^-$  ( $\pi^+$ ) multiplicity is observed when going from the  $NL$  (or  $DDF$ ) to the  $NL\rho$  and then to the  $NL\rho\delta$  model, i.e. increasing the vector contribution  $f_\rho$  in the isovector channel. This trend is more pronounced for kaons, see the right panel, due to the high density selection of the source and the proximity to the production threshold. The results for the  $DDF$  model, density dependent couplings with a large  $f_\rho$  decrease at high density, are fully consistent. They are always closer to the  $NL$  case (without isovector interactions) but the difference, still seen for  $\pi^{+,-}$ , is completely disappearing for  $K^{0,+}$ , selectively produced at high densities.

When isovector fields are included the symmetry potential energy in neutron-rich matter is repulsive for neutrons and attractive for protons. In a *HIC* this leads to a fast, pre-equilibrium, emission of neutrons. Such a *mean field* mechanism, often referred to as isospin fractionation [1, 2], is responsible for a reduction of the neutron to proton ratio during the high density phase, with direct consequences on particle production in inelastic  $NN$  collisions.

*Threshold* effects represent a more subtle point. The energy conservation in a hadron collision in general has to be formulated in terms of the canonical momenta, i.e. for a reaction  $1 + 2 \rightarrow 3 + 4$  as  $s_{in} = (k_1^\mu + k_2^\mu)^2 = (k_3^\mu + k_4^\mu)^2 = s_{out}$ . Since hadrons are propagating with effective (kinetic) momenta and masses, an equivalent relation should be formulated starting from the effective

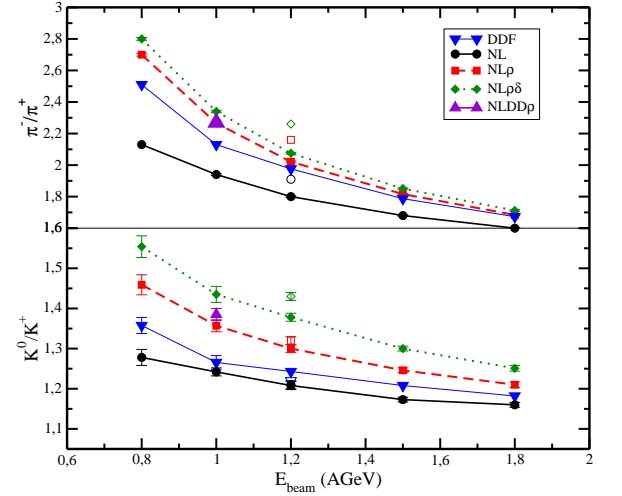


FIG. 6:  $\pi^-/\pi^+$  (upper) and  $K^0/K^+$  (lower) ratios as a function of the incident energy for the same reaction and models as in Fig. 5. In addition we present, for  $E_{beam} = 1$  AGeV,  $NL\rho$  results with a density dependent  $\rho$ -coupling (triangles), see text. The *open* symbols at 1.2 AGeV show the corresponding results for a  $^{132}Sn + ^{124}Sn$  collision, more neutron rich.

in-medium quantities  $k^{*\mu} = k^\mu - \Sigma^\mu$  and  $m^* = m + \Sigma_s$ , where  $\Sigma_s$  and  $\Sigma^\mu$  are the scalar and vector self-energies, Eqs.(4). In reactions where nucleon resonances, especially the different isospin states of the  $\Delta$  resonance, and hyperons enter, also their self energies are relevant for energy conservation. We specify them in the usual way according to the light quark content and with appropriate Clebsch-Gordon coefficients [33]. The self-energy contribution to the energy conservation in inelastic channels will influence the particle production in two different ways. On one hand it will directly determine the thresholds and thus the multiplicities of a certain type of particles, in particular of the sub-threshold ones, as here for the kaons. Secondly it will modify the phase space available in the final channel.

In fact in neutron-rich systems *mean field* and *threshold* effects are acting in opposite directions on particle production and might compensate each other. As an example,  $nn$  collisions excite  $\Delta^{-,0}$  resonances which decay mainly to  $\pi^-$ . In a neutron-rich matter the mean field effect pushes out neutrons making the matter more symmetric and thus decreasing the  $\pi^-$  yield. The threshold effect on the other hand is increasing the rate of  $\pi^-$ 's due to the enhanced production of the  $\Delta^-$  resonances: now the  $nn \rightarrow p\Delta^-$  process is favored (with respect to  $pp \rightarrow n\Delta^{++}$ ) since more effectively a neutron is converted into a proton. Such interplay between the two mechanisms cannot be fully included in a non-relativistic dynamics, in particular in calculations where the baryon symmetry potential is treated classically [46, 47].

In the 0.8 – 1.8 AGeV range the sensitivity is larger for the  $K^0/K^+$  compared to the  $\pi^-/\pi^+$  ratio, as we can



see from Fig.6. This is due to the subthreshold production and to the fact that isospin effects enter twice in the two-steps production of kaons, [48]. Between the two extreme  $DDF$  and  $NL\rho\delta$  isovector interaction models, the variations in the ratios are of the order of 14 – 16% for kaons, while they reduce to about 8 – 10% for pions. Interestingly the Iso- $EoS$  effect for pions is increasing at lower energies, when approaching the production threshold. We have to note that in a previous study of kaon production in excited nuclear matter the dependence of the  $K^0/K^+$  yield ratio on the effective isovector interaction appears much larger (see Fig.8 of ref.[33]). The point is that in the non-equilibrium case of a heavy ion collision the asymmetry of the source where kaons are produced is in fact reduced by the  $n \rightarrow p$  “transformation”, due to the favored  $nn \rightarrow p\Delta^-$  processes. This effect is almost absent at equilibrium due to the inverse transitions, see Fig.3 of ref.[33]. Moreover in infinite nuclear matter even the fast neutron emission is not present. This result clearly shows that chemical equilibrium models can lead to uncorrect results when used for transient states of an *open* system. In the same Fig. 6 we also report results at 1.2 AGeV for the  $^{132}\text{Sn} + ^{124}\text{Sn}$  reaction, induced by a radioactive beam, with an overall larger asymmetry (open symbols). The isospin effects are clearly enhanced.

## VI. TESTING DECONFINEMENT AT HIGH ISOSPIN DENSITY

The hadronic matter is expected to undergo a phase transition into a deconfined phase of quarks and gluons at large densities and/or high temperatures. On very general grounds, the transition’s critical densities are expected to depend on the isospin of the system, but no experimental tests of this dependence have been performed so far. Moreover, up to now, data on the phase transition have been extracted from ultrarelativistic collisions, when large temperatures but low baryon densities are reached. In order to check the possibility of observing some precursor signals of some new physics even in collisions of stable nuclei at intermediate energies we have performed some event simulations for the collision of very heavy, neutron-rich, elements. We have chosen the reaction  $^{238}\text{U} + ^{238}\text{U}$  (average proton fraction  $Z/A = 0.39$ ) at 1 AGeV and semicentral impact parameter  $b = 7\text{ fm}$  just to increase the neutron excess in the interacting region. To evaluate the degree of local equilibration and the corresponding temperature we have followed the momentum distribution in a space cell located in the c.m. of the system; in the same cell we report the maximum mass density evolution. Results are shown in Fig. 7. We see that after about 10 fm/c a nice local equilibration is achieved. We have a unique Fermi distribution and from a simple fit we can evaluate the local temperature. At this beam energy the maximum density coincides with the thermalization, then the system is quickly cooling while expanding. In Fig.7, lower panel, we report the

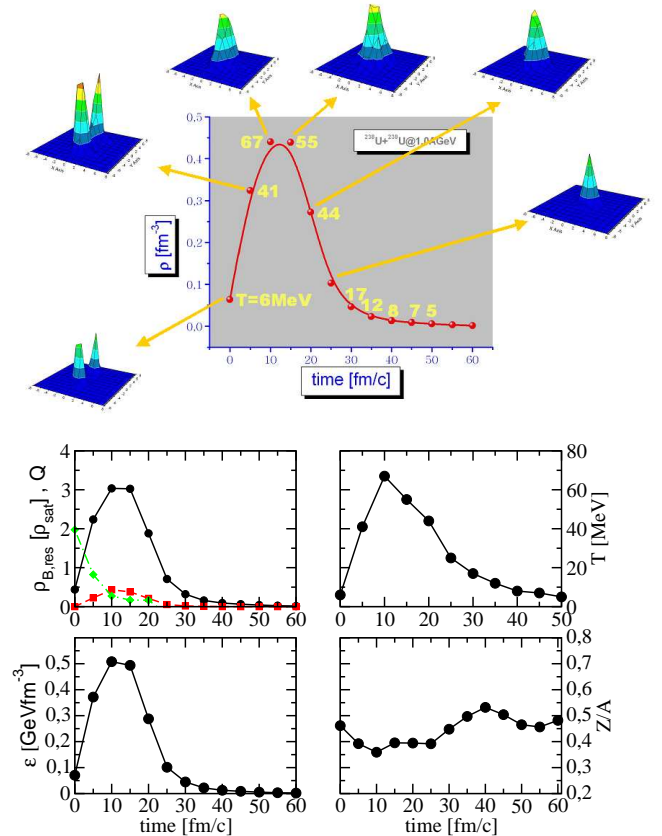


FIG. 7: Uranium-Uranium 1 AGeV semicentral. Correlation between density, temperature, momentum thermalization inside a cubic cell 2.5 fm wide, located in the center of mass of the system. Lower panel: density, temperature, energy density, momentum, proton fraction. Curves in the upper-left: black dots - baryon density in  $\rho_0$  units; grey dots - quadrupole moment in momentum space; squares - resonance density.

time evolution of all physics parameters inside the c.m. cell in the interaction region.. We note that a rather exotic nuclear matter is formed in a transient time of the order of 10 fm/c, with baryon density around 3 – 4 $\rho_0$ , temperature 50 – 60 MeV, energy density 500 MeV fm<sup>-3</sup> and proton fraction between 0.35 and 0.40, well inside the estimated mixed phase region, see the following..

A study of the isospin dependence of the transition densities has been performed up to now, to our knowledge, only by Mueller [49]. The conclusion is that, moving from symmetric nuclei to nuclei having  $Z/A \sim 0.3$ , the critical density is reduced by roughly 10%. Here we explore in a more systematic way the model parameters and we estimate the possibility of forming a mixed-phase of quarks and hadrons in experiments at energies of the order of a few GeV per nucleon.

Concerning the hadronic phase, we use the rela-

tivistic non-linear Walecka-type model of Glendenning-Moszkowski (*GM...*) [50], where the isovector part is treated just with  $\rho$ -meson couplings, and the iso-stiffer  $NL\rho\delta$  interaction [51].

For the quark phase we consider the *MIT* bag model [52] with various bag pressure constants. In particular we are interested in those parameter sets which would allow the existence of quark stars [53, 54], i.e. parameters sets for which the so-called Witten-Bodmer hypothesis is satisfied [55, 56]. One of the aim of our work it to show that if quark stars are indeed possible, it is then very likely to find signals of the formation of a mixed quark-hadron phase in intermediate-energy heavy-ion experiments [51].

The scenario we would like to explore corresponds to the situation realized in experiments at moderate energy, in which the temperature of the system is at maximum of the order of a few ten *MeV*. In this situation, only a tiny amount of strangeness can be produced and therefore we can only study the deconfinement transition from hadron matter into up and down quark matter. Since there no time for weak decays the environment is rather different from the neutron star case.

### Mixed phase

The structure of the mixed phase is obtained by imposing the Gibbs conditions [59, 60] for chemical potentials and pressure and by requiring the conservation of the total baryon and isospin densities

$$\begin{aligned}\mu_B^{(H)} &= \mu_B^{(Q)}, \quad \mu_3^{(H)} = \mu_3^{(Q)}, \\ P^{(H)}(T, \mu_{B,3}^{(H)}) &= P^{(Q)}(T, \mu_{B,3}^{(Q)}), \\ \rho_B &= (1 - \chi)\rho_B^H + \chi\rho_B^Q, \\ \rho_3 &= (1 - \chi)\rho_3^H + \chi\rho_3^Q,\end{aligned}\quad (7)$$

where  $\chi$  is the fraction of quark matter in the mixed phase. In this way we get the *binodal* surface which gives the phase coexistence region in the  $(T, \rho_B, \rho_3)$  space [49, 60]. For a fixed value of the conserved charge  $\rho_3$ , related to the proton fraction  $Z/A \equiv (1 + \rho_3/\rho_B)/2$ , we will study the boundaries of the mixed phase region in the  $(T, \rho_B)$  plane. We are particularly interested in the lower baryon density border, i.e. the critical/transition density  $\rho_{cr}$ , in order to check the possibility of reaching such  $(T, \rho_{cr}, \rho_3)$  conditions in a transient state during an *HIC* at relativistic energies. In the hadronic phase the charge chemical potential is given by  $\mu_3 = 2E_{sym}(\rho_B)\frac{\rho_3}{\rho_B}$ . Thus, we expect critical densities rather sensitive to the isovector channel in the hadronic *EoS*.

We compare the predictions on the transition to a deconfined phase of the two effective Lagrangians *GM3* and *NL\rho\delta*. The isoscalar part is very similar while the isovector *EoS* is different, because in *GM3* we only have the coupling to the vector  $\rho$ -field. In Fig. 8 we show the crossing density  $\rho_{cr}$  separating nuclear matter from the quark-nucleon mixed phase, as a function of the proton

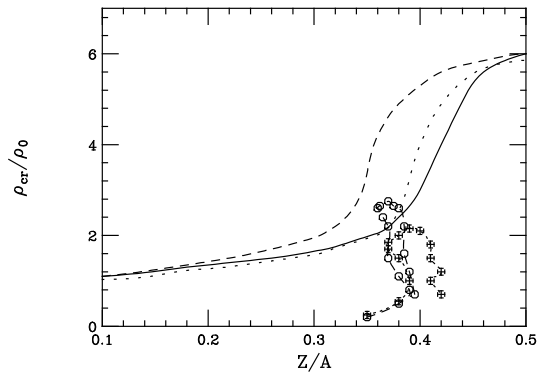


FIG. 8: Variation of the transition density with proton fraction for various hadronic *EoS* parameterizations. Dotted line: *GM3* parametrization; dashed line: *NL\rho* parametrization; solid line: *NL\rho\delta* parametrization. For the quark *EoS*, the *MIT* bag model with  $B^{1/4}=150$  *MeV*. The points represent the path followed in the interaction zone during a semi-central  $^{132}\text{Sn}+^{132}\text{Sn}$  collision at 1 *AGeV* (circles) and at 300 *AMeV* (crosses), see text.

fraction  $Z/A$ . We can see the effect of the  $\delta$ -coupling towards an *earlier* crossing due to the larger symmetry repulsion at high baryon densities. The  $\delta$ -exchange potential provides an extra isospin repulsion of the hadron *EoS*, and its effect shows up in a further reduction of the critical density.

In the same figure we report the paths in the  $(\rho, Z/A)$  plane followed in the c.m. region during the collision of the n-rich  $^{132}\text{Sn}+^{132}\text{Sn}$  system, at different energies. We see that already at 300 *AMeV* we are reaching the border of the mixed phase, and we are well inside it at 1 *AGeV*.

### Deconfinement Precursors

Statistical fluctuations could help in reducing the density at which drops of quark matter form. The reason is that a small bubble can be energetically favored if it contains quarks whose  $Z/A$  ratio is *smaller* than the average value of the surrounding region. This is again due to the strong  $Z/A$  dependence of the free energy, which favors clusters having a small electric charge. These configurations can easily transform into a bubble of quarks having the same flavor content of the original hadrons, even if the density of the system is not large enough to allow deconfinement in the absence of statistical fluctuations. Moreover, since fluctuations favor the formation of bubbles having a smaller  $Z/A$ , neutron emission from the central collision area should be suppressed, what could give origin to specific signatures of the mechanism described in this paper. This corresponds to a *neutron trapping* effect, supported also by a symmetry energy difference in the two phases. In fact while in the hadron phase we have a large neutron potential repulsion (in particular in the *NL\rho\delta* case), in the quark phase we only have the much



smaller kinetic contribution. If in a pure hadronic phase neutrons are quickly emitted or “transformed” in protons by inelastic collisions, when the mixed phase starts forming, neutrons are kept in the interacting system up to the subsequent hadronization in the expansion stage [51]. Observables related to such neutron “trapping” could be an inversion in the trend of the formation of neutron rich fragments and/or of the  $\pi^-/\pi^+$ ,  $K^0/K^+$  yield ratios for reaction products coming from high density regions, i.e. with large transverse momenta. In general we would expect a modification of the rapidity distribution of the emitted “isospin”, with an enhancement at mid-rapidity joint to large event by event fluctuations. A more detailed analysis is clearly needed.

## VII. PERSPECTIVES

We have shown in few examples the richness of the physics we can describe using mean field transport equations, inspired by the pioneering works of David M. Brink. We have seen that collisions of n-rich heavy ions from low to intermediate energies can bring new information on the isovector part of the in-medium interaction in different regions of high baryon densities, qualitatively different from equilibrium *EoS* properties. We have presented quantitative results for charge equilibration in fusion/deep inelastic reactions, differential collective flows and yields of charged pion and kaon ratios. Important non-equilibrium effects for particle production are stressed. Finally our study supports the possibility of observing precursor signals of the phase transition to a

mixed hadron-quark matter at high baryon density in the collision, central or semi-central, of neutron-rich heavy ions in the energy range of a few *GeV* per nucleon. As signatures we suggest to look at observables particularly sensitive to the expected different isospin content of the two phases, which leads to a neutron trapping in the quark clusters. The isospin structure of hadrons produced at high transverse momentum should be a good indicator of the effect.

Many new ideas for fundamental experiments with radioactive beams are emerging. My picture of David Brink like a tree always starting new braches is more and more confirmed.....

## Acknowledgements

I would like to warmly mention the great experience of collaborating with exceptional people on the topics and projects shortly discussed here. I will try to list some of them: V.Baran, M.Colonna, A.Drago, T.Gaitanos, V.Greco, A.Lavagno, B.Liu, M.Pfabe, H.H.Wolter, S.Yildirim and the essential young contributors L.Bonanno, G.Ferini, R.Lionti, N.Pellegriti, V.Prassa, J.Rizzo and E.Santini.

The interaction with experimental groups has been essential, in particular I like to thank the DIPOLE Collab. (D.Pierroutsakou et al.), the CHIMERA Collab. (A.Pagano et al.), and the FOPI Collab. (W.Reisdorf et al.) for the intense discussions and the access to the data.

- 
- [1] B.A. Li, W.U. Schroeder (Eds.), *Isospin Physics in Heavy-Ion Collisions at Intermediate Energies*, Nova Science, New York, 2001.
  - [2] V.Baran, M.Colonna, V.Greco, M.Di Toro, *Phys. Rep.* **410** (2005) 335.
  - [3] P. Chomaz, M. Di Toro, A.Smerzi, *Nucl. Phys.* **A563** (1993) 509.
  - [4] P. F. Bortignon et al., *Nucl. Phys.* **A583** (1995) 101c.
  - [5] S. Flibotte et al., *Phys. Rev. Lett.* **77** (1996) 1448.
  - [6] M. Cinausero et al., *Nuovo Cimento* **111** (1998) 613.
  - [7] D. Pierroutsakou et al., *Eur. Phys. Jour.* **A16** (2003) 423, *Nucl. Phys.* **A687** (2003) 245c.
  - [8] F.Amorini et al., *Phys. Rev.* **C69** (2004) 014608.
  - [9] D. Pierroutsakou et al., *Phys. Rev.* **C71** (2005) 054605.
  - [10] D. M. Brink and M. Di Toro, *Nucl. Phys.* **A372** (1981) 151.
  - [11] V. Baran et al., *Nucl. Phys.* **A600** (1996) 111.
  - [12] M.Cabibbo et al., *Nucl. Phys.* **A637** (1998) 374.
  - [13] V. Baran et al., *Nucl. Phys.* **A679** (2001) 373.
  - [14] C. Simenel et al., *Phys. Rev. Lett.* **86** (2000) 2971.
  - [15] V. Baran, D. M. Brink, M. Colonna, M. Di Toro, *Phys. Rev. Lett.* **87** (2001) 182501
  - [16] D.Pierroutsakou et al., LNS exp. proposal 2006, PAC approved.
  - [17] L. Bonanno, *Effetti di radiazione diretta dipolare sulla sintesi degli elementi superpesanti*, Master Thesis, Catania Univ. 2004.
  - [18] A letter of intent for the new SPIRAL2 facility at GANIL is in preparation.
  - [19] B. D. Serot, J. D. Walecka, *Advances in Nuclear Physics*, **16**, 1, eds. J. W. Negele, E. Vogt, (Plenum, N.Y., 1986).
  - [20] C. M. Ko, Q. Li, R. Wang, *Phys. Rev. Lett.* **59** (1987) 1084.
  - [21] B. Blättel, V. Koch, U. Mosel, *Rep. Prog. Phys.* **56** (1993) 1.
  - [22] S. Kubis, M. Kutschera, *Phys. Lett.* **B399** (1997) 191.
  - [23] B. Liu, V. Greco, V. Baran, M. Colonna, M. Di Toro, *Phys. Rev.* **C65** (2002) 045201.
  - [24] T. Gaitanos, M. Di Toro, S. Typel, V. Baran, C. Fuchs, V. Greco, H.H. Wolter, *Nucl. Phys.* **A732** (2004) 24.
  - [25] F. de Jong, H. Lenske, *Phys. Rev.* **C57** (1998) 3099; E.N.E. van Dalen, C. Fuchs, A. Faessler, *Nucl. Phys.* **A744** (2004) 227.
  - [26] E.N.E. van Dalen, C. Fuchs, A. Faessler, *Phys. Rev. Lett.* **95** (2005) 022302.
  - [27] M. Di Toro, M. Colonna, J. Rizzo, AIP Conf. Proc., Vol.**791** (2005) 70-83.
  - [28] J. Rizzo, M. Colonna, M. Di Toro, *Phys. Rev.* **C72** (2005)

- 064609.
- [29] P. Danielewicz, Roy A. Lacey, et al., *Phys. Rev. Lett.* **81**, (1998) 2438;  
C. Pinkenburg *et al.*, *Phys. Rev. Lett.* **83**, (1999) 1295.
  - [30] T. Gaitanos, C. Fuchs, H.H. Wolter, A. Faessler, *Eur. Phys. J. A* **12** (2001) 421;  
T. Gaitanos, C. Fuchs, H.H. Wolter, *Nucl. Phys.* **A741** (2004) 287.
  - [31] C. Fuchs, H.H. Wolter, *Nucl. Phys.* **A589** (1995) 732.
  - [32] H. Huber, J. Aichelin, *Nucl. Phys.* **A573** (1994) 587.
  - [33] G. Ferini, M. Colonna, T. Gaitanos, M. Di Toro, *Nucl. Phys.* **A762** (2005) 147.
  - [34] V. Greco, V. Baran, M. Colonna, M. Di Toro, T. Gaitanos, H.H. Wolter, *Phys. Lett.* **B562** (2003) 215.
  - [35] J.Y. Ollitrault, *Phys. Rev.* **D46** (1992) 229.
  - [36] P. Danielewicz, *Nucl. Phys.* **A673** (2000) 375.
  - [37] B.A. Li and A.T. Sustich, *Phys. Rev. Lett.* **82** (1999) 5004.
  - [38] B.A. Li, *Phys. Rev. Lett.* **85** (2000) 4221.
  - [39] R. Stock, *Phys. Rep.* **135** (1986) 259.
  - [40] J. Aichelin, C.M. Ko, *Phys. Rev. Lett.* **55** (1985) 2661.
  - [41] C. Fuchs, *Prog.Part.Nucl.Phys.* **56** 1-103 (2006).
  - [42] C.Hartnack, H.Oeschler, J.Aichelin, *Phys. Rev. Lett.* **96** (2006) 012302.
  - [43] W. Cassing, L.Tolos, E.L. Bratkovskaya, A. Ramos, *Nucl. Phys.* **A727** 59 (2003).
  - [44] H. Weber, E.L. Bratkovskaya, W. Cassing, H. Stöcker, *Phys. Rev.* **C67** 014904 (2003).
  - [45] T.Klähn et al. *Constraints on the high-density nuclear equation of state ...*, *arXiv:nucl-th/0602038*.
  - [46] B.A. Li, G.C. Yong, W. Zuo, *Phys. Rev.* **C71** 014608 (2005).
  - [47] Q. Li et al., *Phys. Rev.* **C72** 034613 (2005).
  - [48] In the energy range explored here, the main contribution to the kaon yield comes from the pionic channels, in particular from  $\pi N$  collisions, and from the  $N\Delta$  channel, which together account for nearly 80% of the total yield, see [33].
  - [49] H.Mueller, *Nucl. Phys.* **A618** (1997) 349.
  - [50] N.K.Glendenning, S.A.Moszkowski, *Phys. Rev. Lett.* **67** (1991) 2414.
  - [51] M. Di Toro, A. Drago, T. Gaitanos, V. Greco, A. Lavagno, *Testing Deconfinement...*, *nucl-th/0602052*, *Nucl. Phys.* **A** (2006) in press.
  - [52] A.Chodos et al., *Phys. Rev.* **D9** (1974) 3471.
  - [53] P.Haensel, J.L.Zdunik, R.Schaeffer, *Astron. Astrophys.* **160** (1986) 121.
  - [54] A.Drago, A.Lavagno, *Phys. Lett.* **B511** (2001) 229.
  - [55] E.Witten, *Phys. Rev.* **D30** (1984) 272.
  - [56] A.R.Bodmer, *Phys. Rev.* **D4** (1971) 1601.
  - [57] M.Alford, S.Reddy, *Phys. Rev.* **D67** (2003) 074024.
  - [58] A.Drago, A.Lavagno, G.Pagliara, *Phys.Rev.* **D69** (2004) 057505.
  - [59] L.D.Landau, L.Lifshitz, *Statistical Physics*, Pergamon Press, Oxford 1969.
  - [60] N.K.Glendenning, *Phys. Rev.* **D46** (1992) 1274.